This is a preprint, the final version is subject to change, of the American Mineralogist (MSA)
Cite as Authors (Year) Title. American Mineralogist, in press.
(DOI will not work until issue is live.) DOI: http://dx.doi.org/10.2138/am.2013.4318

A computational model of cation ordering in the magnesioferrite-qandilite ($MgFe_2O_4$-Mg_2TiO_4) solid solution and its potential application to titanomagnetite (Fe_3O_4-Fe_2TiO_4)

Richard J. Harrison[1], Erika J. Palin[11] and Natasha Perks[2]

1. Department of Earth Sciences, University of Cambridge, Downing Street, Cambridge, CB2 3EQ, U.K. (rjh40@esc.cam.ac.uk)
2. Department of Physics, University of Oxford, Parks Road, Oxford, OX1 3PU, U.K.

ABSTRACT

Cation ordering in the magnesioferrite-qandilite ($MgFe_2O_4$-Mg_2TiO_4) solid solution has been investigated using an interatomic potential model combined with Monte Carlo simulations. The dominant chemical interaction controlling the thermodynamic mixing behaviour of the solid solution is a positive nearest-neighbour pairwise interaction between tetrahedrally coordinated Fe^{3+} and octahedrally coordinated Ti^{4+} (J_{FeTi}^{TO}). The predicted cation distribution evolves gradually from the Néel-Chevalier model to the Akimoto model as a function of increasing J_{FeTi}^{TO}, with J_{FeTi}^{TO} = 1000 ± 100 K providing an adequate description of both the temperature and composition dependence of the cation distribution and the presence of a miscibility gap. Although Mg is a good analague of Fe^{2+} in endmember spinels, a comparison of model predictions for $MgFe_2O_4$-Mg_2TiO_4 with observed cation ordering behaviour in titanomagnetite (Fe_3O_4-Fe_2TiO_4) demonstrates that the analogue breaks down for Fe_3O_4-rich compositions, where a value of J_{FeTi}^{TO} closer to zero is needed to explain the observed cation distribution. It is proposed that screening of Ti^{4+} by mobile charge carriers on the octahedral sublattice is responsible for the dramatic reduction in J_{FeTi}^{TO}. If confirmed, this conclusion will have significant implications for attempts to create a realistic thermodynamic model of titanomagnetite.

[1] Present address: Meteorological Office Hadley Centre, FitzRoy Road, Exeter EX1 3PB, U.K.

Keywords: Magnesioferrite, qandilite, titanomagnetite, cation distribution, computer simulations

INTRODUCTION

The titanomagnetite solid solution between magnetite (Fe_3O_4) and ulvöspinel (Fe_2TiO_4) is the dominant carrier of magnetic remanence in nature, and is of central importance to paleomagnetic, rock magnetic and mineral magnetic studies. Both endmembers adopt the cubic inverse spinel structure at room temperature, with cations occupying two distinct types of crystallographic stite (tetrahedral and octahedral). The distribution of Fe^{3+}, Fe^{2+} and Ti^{4+} cations between tetrahedral and octahedral sites has a profound impact on the intrinsic magnetic properties of titanomagnetite. The presence of tetrahedral Fe^{2+} is of particular importance, as this has been linked to large increases in both magnetocrystalline anisotropy and magnetostriction due to a dynamic Jahn-Teller distortion (Kąkol et al. 1991a and b; Church et al. 2011). However, despite numerous studies performed over many years with a range of increasingly sophisticated analysis techniques (see Pearce et al. 2010 for a review), there is still no consensus regarding the temperature and composition dependence of the cation distribution in titanomagnetite. For example, two of the most recent and detailed studies (Bosi et al. 2009 using X-ray single crystal diffraction and Pearce et al. 2010 using X-ray magnetic circular dichroism) present results that are at opposite extremes of the range of previously reported cation distributions and that disagree dramatically in their assessment of when Fe^{2+} first enters the tetrahedral site.

A complicating factor in titanomagnetite is that Fe^{2+} and Fe^{3+} differ only by a single, highly mobile 3d electron, which not only makes distinguishing the two cations an experimental challenge but also makes computational studies more difficult due to the problem of deciding how the excess electron density associated with Fe^{2+} should be distributed across the available Fe sites. Given these complexities, it becomes a worthwhile exercise to consider the magnesioferrite-qandilite ($MgFe_2O_4$-Mg_2TiO_4) solid solution – a potential analogue of titanomagnetite in which the Fe^{2+} cation is entirely replaced by Mg^{2+}. It has long been established that Mg^{2+} is a good analogue for Fe^{2+} in endmember spinels, with the substitution of Mg^{2+} for Fe^{2+} having little effect on temperature-dependent cation distributions (Harrison and Putnis 1999a) and spinel solid solutions involving exchange of Mg^{2+} and Fe^{2+} behaving in a manner that is close to ideal (Trestman-Matts et al. 1984; Nell et al. 1989; Andreozzi and Lucchesi 2002; Palin and Harrison 2007a). The $MgFe_2O_4$-Mg_2TiO_4

solid solution offers, therefore, the possibility to study cation ordering in a system that is closely analogous to titanomagnetite, yet (a) allows the distribution of Mg^{2+} and Fe^{3+} cations to be determined reliably using X-ray powder diffraction, (b) permits the high-temperature distribution to be quenched without significant cation redistribution, (c) enables sample synthesis and analysis to be performed in air at high temperatures without fear of oxidation and (d) lacks the computational complexities associated with mobile electronic charge.

The main focus of this paper is the development of an atomistic model of cation ordering in $MgFe_2O_4$-Mg_2TiO_4. The computational approach, outlined in Section 1, builds on that developed by Palin and Harrison (2007b) and Palin et al. (2008) for the endmembers $MgFe_2O_4$ and Mg_2TiO_4, combined with the extension of the method to binary spinel solid solutions by Palin and Harrison (2007a). Application of the method to $MgFe_2O_4$-Mg_2TiO_4 is described in Section 2. Comparisons between $MgFe_2O_4$-Mg_2TiO_4 and Fe_3O_4-Fe_2TiO_4 are made in Section 3, and the possible reasons for the observed differences between the two systems are explored. Our conclusions provide new insight into the nature of cation ordering in titanomagnetite, and point the way forward for future computational studies of this important magnetic mineral.

1. Development of the Atomistic Model

1.1 Theory

The atomistic model used here is based on the *J* formalism described by Bosenick et al. (2001) and Palin and Harrison (2007b). The total energy, E, of a network of interacting cations can be expressed as a sum of pairwise cation-cation interaction energies. For two species A and B mixing on a network of identical sites, $E = N_{AA}E_{AA} + N_{BB}E_{BB} + N_{AB}E_{AB}$, where E_{AA}, E_{BB} and E_{AB} are the energies associated with A–A, B–B, and A–B neasest neighbour pairs, and N_{AA}, N_{BB}, and N_{AB} are the number of A–A, B–B, and A–B pairs in the network. The interdependence of N_{AA}, N_{BB} and N_{AB} allows this expression to be rewritten solely in terms of the number of unlike cation pairs in the network, $E = E_0 + N_{AB}J$, where E_0 is a constant and $J = E_{AB} - 1/2(E_{AA} + E_{BB})$. The sign of J determines the ordering behaviour of the A and B cations: positive values favour A–A and B–B neighbours, leading to chemical clustering; negative values favour A–B neighbours, leading to cation ordering. Interaction parameters describing the energy more distant neighbour pairs can be defined in the same way and summed to give the total energy of the system. In the case of spinel,

where cations are distributed across two networks of symmetrically distinct sites (i.e. the tetrahedral [T] and octahedral [O] sublattices), an additional site preference energy (a.k.a. chemical potential, μ) is required to complete the total energy. Chemical potential terms can be written $E = \mu N_A^T$, where N_A^T is the number of A atoms sitting on the T sublattice. The sign of μ dictates the site preference of A: a positive value indicates an O site preference, a negative value a T site preference. Using static lattice empirical potential calculations, Palin and Harrison (2007b) determined μ and J for T-T, O-O and T-O interactions out to 4th nearest neighbours in a range of 2-3 endmember spinels, including $MgFe_2O_4$. Using a combination of static lattice empirical potential and ab initio calculations, Palin et al. (2008) performed a similar exercise for the 2-4 spinel Mg_2TiO_4. The extension of the J formalism to the binary spinel solid solution $MgAl_2O_4$-$FeAl_2O_4$ is described by Palin and Harrison (2007a). Adaptation of this method to $MgFe_2O_4$-Mg_2TiO_4 is described below.

Magnesioferrite-qandilite $(MgFe_2O_4)_{1-M}(Mg_2TiO_4)_M$ is a binary system consisting of two inverse spinels. The cation distribution between T and O sites can be written as:

	T	O	Sum
Mg^{2+}	$1 - x - y$	$M + x + y$	$1 + M$
Fe^{3+}	x	$2 - 2M - x$	$2 - 2M$
Ti^{4+}	y	$M - y$	M
Sum	1	2	3

where x and y are cation distribution parameters and M is the mole fraction of Mg_2TiO_4. As shown by Palin and Harrison (2007a), the total energy of such a system can formally be expressed as a sum of pairwise cation-cation interaction parameters and chemical potentials:

$$\begin{aligned} E = & N_{MgFe}^{TT} J_{MgFe}^{TT} + N_{MgTi}^{TT} J_{MgTi}^{TT} + N_{FeTi}^{TT} J_{FeTi}^{TT} \\ & + N_{MgFe}^{OO} J_{MgFe}^{OO} + N_{MgTi}^{OO} J_{MgTi}^{OO} + N_{FeTi}^{OO} J_{FeTi}^{OO} \\ & + N_{MgFe}^{TO} J_{MgFe}^{TO} + N_{MgTi}^{TO} J_{MgTi}^{TO} + N_{FeTi}^{TO} J_{FeTi}^{TO} \\ & + \mu_x x + \mu_y y + \mu_M M \\ & + E_0 \end{aligned} \quad (1)$$

where N_{MgFe}^{TT}, etc., is the number of Mg^{2+}-Fe^{3+} cation pairs of a given type and J_{MgFe}^{TT}, etc., is the corresponding interaction parameter. E_0 is a constant that plays no role in determining the cation distribution. There is a chemical potential term corresponding to each of the independent variables defining the cation distribution (x, y and M). The μ_M chemical potential produces a linear variation of total energy with bulk composition of the system, and plays no role in determining either the cation distribution or the excess thermodynamic mixing properties of the solid solution. The choice of variables x and y to describe the cation distribution is somewhat arbitrary. However, since Fe^{3+} and Ti^{4+} are absent from the Mg_2TiO_4 and $MgFe_2O_4$ endmembers, respectively, this choice allows μ_x and μ_y to be equated with the chemical potentials already determined for each endmember. Implicit in Eqn. 1 is that interactions are summed over 1st, 2nd, 3rd and 4th nearest neighbour interactions, as described by Palin and Harrison (2007b).

1.2 Determination of the solid solution J parameters

The only energy terms in Eqn. 1 that are not already known from studies of the endmembers are the Fe^{3+}-Ti^{4+} cation-cation interaction parameters J_{FeTi}^{TT}, J_{FeTi}^{OO} and J_{FeTi}^{TO}. As with our previous work, static lattice energy calculations using empirical interatomic potentials are used to estimate values for the unknown Js. The interatomic potentials have the Buckingham form:

$$E = A\exp(-r/\rho) - \frac{C}{r^6} \quad (2)$$

where A, ρ and C are constants, and the value of A depends on the coordination of the atom. Formal charges were used for all species, and the potential parameters used were obtained from previous work on the endmembers $MgFe_2O_4$ and Mg_2TiO_4 (Palin and Harrison 2007b; Palin et al. 2008). We examined 16 different compositions across the join, i.e. M = 0, 1/16…1. A 2x2x2 supercell of the spinel structure was created and the cations were placed randomly on the available T and O sites in proportions appropriate to the chosen values of x, y, and M. Given that the amount of Ti^{4+} on tetrahedral sites is observed by experiment to be negligible at all compositions and temperatures (de Grave et al. 1975), we chose to place Ti^{4+} cations exclusively on the octahedral sublattice (i.e. y = 0). This decision was taken to minimise undue bias in the derived interaction parameters by ensuring that all of the generated configurations were physically achievable by the real system. A

144 total of 217 configurations were created. Each configuration was relaxed with respect to both lattice
145 parameters and atomic positions at constant pressure using the program GULP (Gale 1997, Gale
146 and Rohl 2003). The set of 217 optimised lattice energies were then used to calculate values for all
147 *J*s and μs using the least-squares optimisation method of Bosenick et al. (2001). Given the lack of
148 tetrahedral Ti^{4+}, J_{MgTi}^{TT} and J_{FeTi}^{TT} were not included in the optimisation procedure. All other
149 parameters were allowed to vary.

150 Results of the *J* optimisation procedure are displayed in Fig. 1. The J_{MgTi} and J_{MgFe}
151 parameters obtained here display the same systematics observed in the endmember studies (Palin
152 and Harrison 2007b; Palin et al. 2008). The 1st nearest neighbour interactions are dominant, and all
153 statistically significant interaction parameters are negative, indicating that Mg^{2+}-Ti^{4+} and Mg^{2+}-Fe^{3+}
154 cation pairs are energetically favourable. J_{MgTi} parameters are typically larger than the
155 corresponding J_{MgFe} parameters. This is due to the larger contrast in cation charge for Mg^{2+}-Ti^{4+}
156 pairs compared to Mg^{2+}-Fe^{3+} pairs, which leads to a larger electrostatic contribution to the
157 interaction energy. The values of J_{MgTi} are similar to those obtained by Palin et al. (2008) for
158 endmember Mg_2TiO_4. Value of J_{MgFe}, however, are significantly larger than those reported by Palin
159 and Harrison (2007b) for endmember $MgFe_2O_4$. This is due to the use of a formal charge of -2 for
160 O atoms in this study, rather than the value of -1.65 used by Palin and Harrison (2007b). In the
161 following we adopt the simplest assumption that J_{MgTi} and J_{MgFe} are independent of bulk
162 composition and equal to those derived for the endmembers. This ensures, at least, that the model
163 reproduces the observed endmember behaviour.

164 The optimised results for J_{FeTi} interactions indicate that the dominant interaction in the solid
165 solution is the 1st nearest neighbour interaction between Fe^{3+} cations on tetrahedral sites and Ti^{4+}
166 cations on octahedral sites (referred to from now on as J_{FeTi}^{TO}). All other J_{FeTi} interactions are
167 within two standard deviations of zero. The fitted value of J_{FeTi}^{TO} (1828 ± 286 K) is large and
168 positive, indicating that Fe^{3+}-Ti^{4+} TO pairs are energetically unfavourable and that the system will
169 attempt to minimise the number of such pairs in the solid solution. This result compares favourably
170 with the hematite-ilmenite (Fe_2O_3-$FeTiO_3$) system, where 1st nearest neighbour interactions
171 between Fe^{3+} and Ti^{4+} were also found to be positive (Harrison et al. 2000; Harrison 2006).

172 *J* values extracted using static lattice empirical potential calculations provide valuable
173 insight into the sign and relative importance of different cation-cation interactions, but often

produce only approximate agreement with experimental observations. The prediction that there is only one dominant interaction in the solid solution greatly simplifies attempts to obtain a physically realistic model that reproduces the experimental data. In Section 2 we explore the thermodynamic behaviour of the system as a function of increasing $J_{\mathrm{FeTi}}^{\mathrm{TO}}$ and compare the predicted results with experimental observations to obtain an estimate of the most likely value of this parameter in the real system.

1.3 Monte Carlo Simulations

Monte Carlo (MC) simulations were used to determine the equililibrium cation distribution as a function of temperature and composition, according to the methods outlined by Harrison (2006). A 4x4x4 supercell of the spinel structure was created, containing a total of 1536 cation sites (512 tetrahedral and 1024 octahedral) with periodic boundary conditions. Individual simulations were performed with a fixed bulk composition varying between $0 \leq M \leq 1$ in steps of either 0.1 or 0.2. Starting configurations were created by distributing Ti^{4+} randomly over the octahedral sublattice and then distributing Mg^{2+} and Fe^{3+} randomly over the remaining T and O sites. Note that Ti^{4+} was not constrained to sit exclusively on O sites during the subsequent simulations. Simulations were performed on cooling from 1750 K to 250 K in steps of 250 K. Each simulation ran for a total of 2×10^7 cation swaps (that is, 10^7 equilibration steps and 10^7 production steps).

The J and μ parameters used in the simulations are listed in Table 1. J_{MgTi}, J_{MgFe}, μ_x and μ_y were taken directly from the endmember studies of Palin and Harrison (2007b) and Palin et al. (2008) (note, however, the change in sign of μ_y, since we chose here to define the chemical potential energy using the number of Ti^{4+} cations on T rather than O sites). In both endmember studies, the parameters were optimised to give a good description of the observed ordering behaviour. The only additional parameter used in this study is the 1st nearest-neighbour $J_{\mathrm{FeTi}}^{\mathrm{TO}}$ interaction. Parameters E_0 and μ_M in Eqn. 1 have no effect on the cation distribution or excess thermodynamic properties and were not used in the MC simulations.

2. Application to $MgFe_2O_4$-Mg_2TiO_4

2.1. Cation ordering as a function of temperature, M and J_{FeTi}^{TO}

Simulations were performed for J_{FeTi}^{TO} values ranging from 0 K to 1500 K. In all cases, Ti^{4+} was found almost exclusively on octahedral sites. The maximum amount of Ti^{4+} on tetrahedral sites was $y = 0.026$ (for $T = 1750$ K, $M = 0.8$ and $J_{FeTi}^{TO} = 0$). This amount of tetrahedral Ti^{4+} is consistent with experimental observations of Mg_2TiO_4 at high temperatures (O'Neill et al. 2003). Given that $y \sim 0$, the distribution of all other cations can be defined by a single order parameter, x. We have chosen to summarise the MC results in Fig. 2 by plotting the number of tetrahedral Mg^{2+} cations per formula unit ($Mg^T \sim 1\text{-}x$) as a function of M. Simulated results are shown as black solid lines. The uppermost curve in each figure shows the highest temperature simulation (1750 K), the lowermost curve shows the lowest temperature simulation (250 K).

To aid the discussion, dashed lines in Fig. 2 show four reference cation distribution models. Each of the four models assumes that Ti^{4+} occurs exclusively on octahedral sites. The 'Random' model corresponds to a random distribution of Mg^{2+} and Fe^{3+} across T and O sites. The 'Akimoto' model is analogous to that proposed by Akimoto (1954) for titanomagnetite, and corresponds to a linear variation in tetrahedral Mg^{2+} as a function of M. The 'Kąkol' model is analogous to that proposed by Kąkol et al. (1991b) for titanomagnetite, whereby no tetrahedral Mg^{2+} appears until $M > 0.2$. The 'Néel-Chevalier' model is analagous to that proposed by Néel (1955) and Chevalier et al. (1955) for titanomagnetite, whereby no tetrahedral Mg^{2+} appears until $M > 0.5$.

For $0 \leq J_{FeTi}^{TO} \leq 250$ K, the low-temperature state of the system corresponds to the Néel-Chevalier model (Fig. 2a, b). No Mg^{2+} enters the tetrahedral sites until $M > 0.5$, at which point all octahedral Fe^{3+} is used up and there is no choice but to place additional Mg^{2+} on tetrahedral sites. The tetrahedral preference of Fe^{3+} over Mg^{2+} is a consequence of the negative value of μ_x (Table 1), which dictates that total energy is lowered by increasing tetrahedral Fe^{3+} at the expense of tetrahedral Mg^{2+} (given that Ti^{4+} strongly favours octahedral sites). Increasing temperature leads to increasing Mg^T. For $0 < M \leq 0.5$, the temperature-dependence of Mg^T tracks that observed in endmember $MgFe_2O_4$ (O'Neill et al. 1992; Antao et al. 2005). The temperature dependence of Mg^T diminishes for $M > 0.5$ and disappears entirely for $M > 0.8$.

For $J_{FeTi}^{TO} = 500$ K, there is a marked change in the low-temperature state of the system, with Mg^{2+} entering tetrahedral sites for all $M > 0$ (Fig. 2c). The system adopts a mixed cation distribution that is close to the Néel-Chevalier model for $M > 0.8$ but is closer to the Akimoto model for $M < 0.2$. For $750 \leq J_{FeTi}^{TO} \leq 1000$ K, the low-temperature state moves closer to the

Akimoto model, with an approximately linear variation of Mg^T with M (Fig. 2d-f). For $0 < M < 0.5$ the temperature-dependence of Mg^T is bounded by the Random model at high T and the Akimoto model at low T. For $M > 0.5$, Mg^T remains close to the Akimoto/Random models and there is little temperature dependence (these two models become virtually indistinguishable as M tends to 1). For $J_{FeTi}^{TO} = 1100$ K, the cation distribution follows the Random model for $0.4 \leq M \leq 1$ (Fig. 2g). For $J_{FeTi}^{TO} > 1100$ K we begin to see Mg^T values that exceed the Random model, implying that Mg^{2+} now has a tetrahedral preference relative to Fe^{3+}.

2.2. Comparison with experimental observations

Experimental measurements of the cation distribution in $MgFe_2O_4$-Mg_2TiO_4 have been reported by Tellier (1967) and de Grave et al. (1975). The results of de Grave et al. (1975) are shown in Fig. 3a for two suites of samples: the first was quenched from 1373 K in water (upward triangles) and the second was cooled slowly from 1373 K at a rate of 1 K per minute (downward triangles). Also shown in Fig. 3a are new results from our own experimental work on this system (circles). Details of the experimental work will be presented in detail elsewhere. Samples were synthesised in air at 1400 °C from mixtures of Fe_2O_3 and TiO_2 and then furnace cooled. Cation distributions were obtained by Rietveld refinement of X-ray powder diffraction patterns, and are in excellent agreement with those of de Grave et al. (1975). For $0 \leq M \leq 0.5$, the observed cation distributions fall in between the Random and Akimoto models, with the quenched samples falling closer to the Random model and slowly cooled samples falling closer to the Akimoto model. For $M > 0.5$ the observed cation distribution follows the Random model. Comparing Fig. 3a with the results of MC simulations (Fig. 2), it appears that the atomistic model with $J_{FeTi}^{TO} = 1000 \pm 100$ K provides an adequate description of both the temperature and composition dependence of cation ordering in this system (Fig. 2f). This value of J_{FeTi}^{TO} is of the same order of magnitude as that predicted by the interatomic potential calculations presented in Section 1.2 ($J_{FeTi}^{TO} = 1828 \pm 286$ K).

Perhaps a more rigorous method of presenting the experimental data follows from the thermodynamic model of binary spinel solid solutions described by O'Neill and Navrotsky (1984). Assuming that Ti^{4+} sits on O sites exclusively ($y = 0$), thermodynamic equilibrium with respect to the amount of Fe^{3+} on T sites (x) can be expressed in the form:

$$-RT\ln(K) = \alpha + 2\beta x$$

$$\ln(K) = \ln\left(\frac{x(M+x)}{(1-x)(2-2M-x)}\right) \quad (3)$$

where α and β are coefficients describing the enthalpy variation as a function of x ($H = \alpha x + \beta x^2$). According to Eqn. 3, a plot of $-RT\ln(K)$ vs x should yield a straight line with intercept α and slope 2β. In order to plot the data in this form, we require an estimate for the temperature at which the cation distribution has been equilibrated. For the quenched samples of de Grave et al. (1975) and Tellier (1967) we have assumed that the equilibration temperature is equal to the quench temperature (1373 K). For our own samples and the slowly cooled samples of de Grave et al. (1975) we use an estimated equilibration temperature of 667 K, which corresponds to the temperature at which the observed cation distribution in endmember $MgFe_2O_4$ is equal to the predicted cation distribution according to the thermodynamic model of O'Neill et al. (1992). The resulting plot is shown in Fig. 4a. The dashed line shows the predicted behaviour according to the O'Neill and Navrotsky (1984) model, with the values of α = 26.6 kJ/mol and β = -21.7 kJ/mol obtained by fitting cation distribution data for endmember $MgFe_2O_4$ (O'Neill et al. 1992). Although there is good agreement with the O'Neill-Navrotsky model for $0.7 < x < 1$ (which corresponds mainly to the range of x values in endmember $MgFe_2O_4$), there is dramatic deviation from linear behaviour for $x < 0.7$ (which corresponds mainly to the range of x values in the solid solution). Solid curves in Fig. 4a show the calculated behaviour using the atomistic model with J_{FeTi}^{TO} = 1000 K. The lowermost curve corresponds to highest temperature (1750 K) and the uppermost curve to the lowest temperature (250 K). Agreement between observed and calculated behaviour is much improved with respect to the O'Neill-Navrotsky model. In particular, the predicted curvature of the $-RT\ln(K)$ vs x plot agrees very well with the data of Tellier (1967) (solid squares). Agreement appears to be poorest for small values of x, corresponding to compositions close to Mg_2TiO_4. However, comparing the observed and calculated distributions directly (Fig. 4b), we see that this disagreement is perhaps over emphasised by Eqn. 3.

2.3. Enthalpies of mixing and immiscibility in the solid solution

An independent check of the calibration of the atomistic model can be performed by comparing the calculated and observed enthalpies of mixing (ΔH_{mix}). ΔH_{mix} was calculated by subtracting the MC energy of a mechanical mixture of the endmembers from the MC energy of the solid solution (Fig. 5). At 1750 K (uppermost curve) there is a positive symmetrical enthalpy of mixing that can be described by a regular solution model $\Delta H_{mix} = WM(1\text{-}M)$ with $W = 24$ kJ/mol. As far as we are aware, there are no published reports of ΔH_{mix} data for $MgFe_2O_4$-Mg_2TiO_4. However, in the context of this comparative study, it is useful to compare our predicted curves with recent calorimetric measurements of the titanomagnetite solid solution (Lilova et al. 2012). Drop solution calorimetry data for a suite of titanomagnetites synthesised at 1173 K are plotted as closed circles in Fig. 5. Their data correspond to a regular solution model with $W = 22.60 \pm 8.46$ kJ/mol, which is well within the range of predicted values for the Mg analogue system.

Significant changes in the magnitude, symmetry and curvature of ΔH_{mix} occur at lower simulation temperatures. At 1250 K there is a flattening of the ΔH_{mix} curve and below 1000 K the ΔH_{mix} curves become linear in the central region. This type of behaviour is similar to that observed in simulations of hematite-ilmenite (Harrison et al. 2000) and suggests the presence of a miscibility gap in the solid solution below ~1000 K. Evidence for chemical clustering driven by the positive value of J_{FeTi}^{TO} can be seen in snapshots of the MC similations (Fig. 6). Snaphots are shown for $M = 0.5$ with Mg^{2+} in red, Fe^{3+} in green and Ti^{4+} in blue. At 1750 K there is a random distribution of $MgFe_2O_4$ (red/green) and Mg_2TiO_4 (red/blue) components throughout the simulation cell. At 1000 K and below the distribution becomes increasingly clustered into $MgFe_2O_4$-rich and Mg_2TiO_4-rich regions. The presence of a miscibility gap is also consistent with the thermodynamic model of Sack and Ghiorso (1991), who predicted an asymmetric gap below 883 K for $MgFe_2O_4$-Mg_2TiO_4.

3. Comparison with titanomagnetite

3.1 Cation distributions in titanomagnetite

A summary of recent experimental studies of cation ordering in titanomagnetite is shown in Fig. 3b (Kąkol et al. 1991b; Hamdeh et al. 1999; Bosi et al. 2009; Pearce et al. 2010; Lilova et al. 2012). Unlike $MgFe_2O_4$-Mg_2TiO_4, there is considerable disagreement between different studies. Despite the scatter, however, some important trends emerge. For $M > 0.5$, the average trend falls close to the Akimoto/Random models and there is reasonably good correspondence between the

321 $MgFe_2O_4$-Mg_2TiO_4 and Fe_3O_4-Fe_2TiO_4 systems. For $0 \leq M \leq 0.5$, however, the data fall between
322 the Akimoto and Néel-Chevalier models, with an average trend corresponding approximately to the
323 Kąkol model. The range of scatter is consistent with the in-situ measurements of Trestman-Matts et
324 al. (1983), who found that the cation distribution tends towards the Akimoto model at high T and
325 the Néel-Chevalier model at low T. All of these data deviate markedly from $MgFe_2O_4$-Mg_2TiO_4 in
326 the range $0 \leq M \leq 0.5$ (Fig. 3a), representing a fundamental difference in the behaviour of the two
327 systems.
328 On the basis of the available data, we suggest that $MgFe_2O_4$-Mg_2TiO_4 is a good analogue of
329 Fe_3O_4-Fe_2TiO_4 for $M > 0.5$. The analogue breaks down, however, for $M \leq 0.5$. The analogue
330 between Mg and Fe^{2+} is well established for the endmembers, both from experimental and
331 modelling perspectives (Harrison and Putnis 1999a), with virtually identical values for Mg-Fe^{3+} and
332 Fe^{2+}-Fe^{3+} interaction parameters being determined by Palin and Harrison (2007b). Given the
333 evidence for a large J_{FeTi}^{TO} interaction in $MgFe_2O_4$-Mg_2TiO_4, and the similarity in enthalpies of
334 mixing of the two systems (Fig. 5), we might also expect a J_{FeTi}^{TO} interaction of similar magnitude
335 in Fe_3O_4-Fe_2TiO_4. From Fig. 2, however, it appears that values of $J_{FeTi}^{TO} < 500$ K are needed to
336 reproduce cation distributions close to the Kąkol model and even smaller values (≤ 250 K) are
337 needed to reproduce the Néel-Chevalier model (as required, for example, by the data of Pearce et al.
338 2010). This breakdown points towards some fundamental aspects of the physical behaviour of
339 titanomagnetite that are not accounted for by our atomistic model in its current form. The presence
340 of mobile, delocalised charge carriers in Fe_3O_4-rich titanomagnetite is likely to have a significant
341 impact on the both the equilibrium and kinetic properties of the solid solution. Magnetic ordering
342 may also play an important role at temperatures below 853 K. We now attempt to assess which
343 factors, or combination of factors, can best account for the observed difference between $MgFe_2O_4$-
344 Mg_2TiO_4 and Fe_3O_4-Fe_2TiO_4 for $M \leq 0.5$.
345
346 *3.2. Coupling between cation ordering and magnetic ordering*
347 Both Fe_3O_4 and $MgFe_2O_4$ adopt ferrimagnetic structures below their respective Curie
348 temperatures (T_c). Whereas T_c for stoichiometric Fe_3O_4 is a constant 853 K, T_c for $MgFe_2O_4$ can lie
349 anywhere in the range 550-700 K, depending on the degree of quenched-in cation disorder (O'Neill
350 et al. 1992). Harrison and Putnis (1997) argued that cation ordering and magnetic ordering in

$MgFe_2O_4$ are strongly coupled and that the coupling can be modelled successfully using a mean-field model. They included an energy term in the macroscopic free energy that links the two ordering processes: $E = \lambda x Q_m^2$, where Q_m is the magnetic order parameter and λ is a coupling constant. The sign of the coupling constant is such that an increase in the degree of inversion (x) causes an increase in the degree of magnetic order (i.e. T_c increases with x). Under conditions of global equilibrium with respect to x and Q_m, the opposite must also be true: i.e. when the degree of magnetic order increases on cooling through T_c we expect to see an enhanced degree of inversion. For $MgFe_2O_4$, the kinetics of cation ordering at $T = T_c$ are too slow to allow the onset of magnetic ordering to have any influence on the cation distribution (Harrison and Putnis 1999b). This is not the case for Fe_3O_4, however, where rapid redistribution of Fe^{2+} and Fe^{3+} can occur via electron hopping down to room temperature. Recent experimental observations of natural Fe_3O_4-Fe_2TiO_4 samples with $0.2 < M < 0.4$ (Bowles and Jackson, pers. comm.) provide strong evidence of coupling in the titanomagnetite solid solution.

In deriving the atomistic model we have taken no account of coupling between cation and magnetic ordering processes below T_c. This is justifiable for $MgFe_2O_4$-Mg_2TiO_4, where kinetic limitations prevent global equilibrium with respect to x and Q_m from being achieved on laboratory timescales. It is possible, however, that coupling will lead to enhanced cation order in Fe_3O_4-Fe_2TiO_4, especially for $M < 0.5$, where $T_c > 600$ K and electron hopping is fast enough to respond to the magnetic transition. Incorporation of magnetic ordering into the atomistic model is an obvious next step (Harrison and Becker 2000; Harrison 2006), but is beyond the scope of the current study. Harrison and Putnis (1999a) applied the thermodynamic model of Harrison and Putnis (1997) to cation ordering data for Fe_3O_4 (Wißmann et al. 1998) and demonstrated that the mean-field approach correctly predicts the experimentally observed enhancement of cation order below T_c, implying that coupling in Fe_3O_4 is similar in strength to $MgFe_2O_4$. To demonstrate the magnitude of the effect, we have adapted the macroscopic approach of Harrison and Putnis (1997) to describe a system that behaves like $MgFe_2O_4$ in terms of its equilibrium cation ordering behaviour, but like Fe_3O_4 in terms of its magnetic ordering and kinetic behaviour. The total free energy of the system is written:

$$
\begin{aligned}
&G = \alpha x + \beta x^2 \\
&+RT(x\ln(x)+(1-x)\ln(1-x)+x\ln(x/2)+(2-x)\ln(1-x/2)) \\
&+\frac{1}{2}a_m(T-T_c)Q_m^2+\frac{1}{4}b_mQ_m^4 \\
&+\lambda x Q_m^2
\end{aligned}
\qquad (4)
$$

where the first two lines represent the enthalpy and configurational entropy due to cation ordering (O'Neill and Navrotsky 1983), the third line represents the free energy due to magnetic ordering (Harrison and Putnis 1997), and the fourth line is the coupling term. Minimising G with respect to Q_m at constant x yields:

$$
\begin{aligned}
&Q_m^2 = \frac{b_m}{a_m}(T_c^* - T) \\
&T_c^* = T_c - \frac{2\lambda}{a_m}x
\end{aligned}
\qquad (5)
$$

which represents a second-order magnetic transition with renormalised Curie temperature T_c* that varies linearly with x. A value of λ = -21059 J/mol was obtained by fitting Eqn. 5 to the T_c-x data of O'Neill et al. (1992). A value of T_c = 445 K for the unrenormalised Curie temperature ensures that the equilibrium magnetic transition occurs at 853 K. Values of α = 26.6 kJ/mol and β = -21.7 kJ/mol were taken from O'Neill et al. (1992). A value of a_m = 86.35 J/mol.K^{-1} was calculated from the total magnetic entropy change for a Fe_3O_4-like material containing one Fe^{2+} and two Fe^{3+} cations (ΔS = 1/2 a_m = R[ln 5 + 2 ln 6]). A value of b_m = 80542.5 J/mol is required by the normalisation condition (Q_m = ±1 at 0 K). The dashed line in Fig. 7 shows the cation ordering behaviour that would be observed in the absence of coupling to the magnetic transition. The enhancement of cation order due to coupling is shown by the thick solid line. The maximum difference between the two curves is Δx = 0.06. Even if we make the generous assumption that magnetic ordering could influence the cation distribution by up to ~ 0.1 cations per formula unit, the effect is still a factor of ~2 too small to explain the discrepancy between average cation distributions in $MgFe_2O_4$-Mg_2TiO_4 and Fe_3O_4-Fe_2TiO_4. The effect is completely incapable of accounting for distributions that lie close to the Néel-Chevalier model (e.g. Pearce et al. 2010).

406 *3.3. Compositional dependence of J_{FeTi}^{TO}*

407 By adjusting the value of J_{FeTi}^{TO}, the atomistic model is capable of reproducing the entire
408 range of proposed cation distribution models for titanomagnetite (Fig. 2). Any one particular model
409 can be reproduced by relaxing the assumption that J_{FeTi}^{TO} is a constant for all bulk compositions. To
410 illustrate this concept we have determined the value of J_{FeTi}^{TO} that is needed at each composition to
411 obtain a cation distribution bounded at low T by the Kąkol model (Fig. 8a). This procedure yields a
412 linear increase in J_{FeTi}^{TO} from 250 K at $M = 0.2$ to 1100 K at $M = 0.9$ (closed circles in inset to Fig.
413 8a) and produces a good description of much of the published data.

414 Allowing J_{FeTi}^{TO} to vary as a function of composition provides a powerful means of
415 optimising the parameters of the atomistic model to fit the experimental data. However, this fit is
416 meaningless unless the compositional dependence can be physically justified. There are two main
417 contributions to the cation-cation interaction parameters: a strain contribution resulting from size
418 mismatch between cation pairs and an electrostatic contribution resulting from charge mismatch.
419 Strain interactions can never be screened, and will always be present in a solid solution where
420 cations of different size mix. In systems with large size mismatch (e.g. substitutions involving Mg^{2+}
421 and Ca^{2+} - size mismatch ~28%), it is sometimes necessary to include a composition dependent,
422 configuration independent volume strain energy term when computing J parameters from static
423 lattice energy calculations (Vinograd et al. 2004). In our case, however, Fe^{3+} and Ti^{4+} cations are
424 similar in size (size mismatch ~7%) but differ in charge, and electrostatic interactions are likely to
425 make a larger contribution to J_{FeTi}^{TO} than strain interactions. This is an important statement, since
426 unlike strain interactions, electrostatic interactions may potentially be screened by mobile charge
427 carriers. Fig. 8a provides evidence that J_{FeTi}^{TO} decreases linearly in proportion to the Fe_3O_4 content
428 of the solid solution. We propose that the excess positive charge associated with octahedral Ti^{4+} is
429 gradually screened by an increasing concentration of mobile charge carriers on the octahedral
430 sublattice, thus reducing the electrostatic interaction of octahedral Ti^{4+} with tetrahedral Fe^{3+} in
431 proportion to the Fe_3O_4 content of the solid solution. Sujata and Mason (1992) suggested a similar
432 mechanism to explain the gradual reduction in the activation energy for cation redistribution in
433 ferrospinels $(Fe_3O_4)_z(MeFe_2O_4)_{1-z}$ (Me = Co, Mn, Mg, Ni) with increasing Fe_3O_4 content. For
434 example, the activation energy for Ni diffusion decreases steadily from 3.55 eV for $z = 0.03$ to 2.95
435 eV for $z = 0.14$, 2.6 eV for $z = 0.33$ and 2.08 eV for $z = 0.63$ (Eveno and Paulus 1974). Sujata and

Mason (1992) argue that when the Fe_3O_4 content is large enough, small polaron hopping between Fe^{2+} and Fe^{3+} in ferrospinels can provide local electroneutrality for diffusing ionic species and can effectively screen these species during migration, thereby lowering the activation energy. Spinels that are unable to screen charge in this way display much larger activation energies, and in the case of $MgFe_2O_4$ adopt a very different mechanism of cation ordering (i.e. heterogeneous nucleation and growth instead of homogeneous local diffusion; Walters and Wirtz 1971; Kimura et al. 1977; Harrison and Putnis 1999b).

The proposed screening mechanism appears to be highly effective for compositions close to pure Fe_3O_4, where J_{FeTi}^{TO} is reduced to ~ 0, making the solid solution virtually insensitive to dilute concentrations of Ti^{4+} on the octahedral sublattice. Note that screening of Ti^{4+} is preferred to a charge transfer mechanism, given the lack of any spectroscopic evidence for Ti^{3+} in the solid solution (Pearce et al. 2010). The reduced J_{FeTi}^{TO} leads to a poorer agreement between the calculated and observed enthalpies of mixing (Fig. 8b), although the high T curves are still within error of the experimental data and remain consistent with the presence of a miscibility gap in this system (Price 1981). The anomalous negative enthalpy of mixing for $M \sim 0.2$ is likely due to the fact that reducing J_{FeTi}^{TO} means we no longer account properly for the volume strain energy contribution to the total energy. The agreement seen in Fig. 5 could be restored, however, by addition of a small configuration independent strain energy term of the form suggested by Vinograd et al. (2004).

4. DISCUSSION

4.1. Comment on the merits of atomistic versus macroscopic models

One of the most striking results of this study is the dramatic difference between atomistic and macroscopic models of cation ordering in $MgFe_2O_4$-Mg_2TiO_4 (Fig. 4a). The O'Neill and Navrotsky (1983 and 1984) model (from now on referred to as the O-N model) provides a near perfect description of cation ordering in endmember $MgFe_2O_4$ (O'Neill et al. 1992). Palin and Harrison (2007a) demonstrated from an atomistic perspective that the O-N model correctly captures the thermodynamic consequences of cation ordering in endmember spinels (especially for normal spinels, where short-range order is limited), thereby explaining why it can be applied successfully to such a wide range of systems. It is somewhat suprising, therefore, that the O-N model fails to

account for the rather simple linear relationship between Mg^T and M in the $MgFe_2O_4$-Mg_2TiO_4 solid solution (Fig. 3a). Below we consider possible reasons for the difference between the atomistic and macroscopic approaches to modelling this system, with implications for other systems of this type.

In the O-N model of $MgFe_2O_4$-Mg_2TiO_4, cation ordering in the solid solution is defined by the two energy parameters α and β (Eqn. 3). These two parameters are entirely constrained by cation ordering behaviour in $MgFe_2O_4$; no parameters specific to the solid solution enter the cation distribution model. The mixing properties of the solid solution are defined by a regular solution term of the form $\Delta H_{mix} = WM(1\text{-}M)$ that depends only on bulk composition. The adjustable parameter W allows the enthalpy of mixing and appearence of miscibility gaps to be described, but it does not influence the calculated cation distributions in any way. The parameterisation of the atomistic model is also heavily constrained by cation ordering behaviour in the endmembers. In this study we chose to fix J_{MgFe}, J_{MgTi}, μ_x and μ_y at their endmember values (a procedure that is equivalent to using endmember values of α and β in the O-N model). Inspired by the results of static lattice energy calculations, the mixing properties of the solid solution were then defined by J_{FeTi}^{TO}. This single adjustable parameter plays a similar role to W in the O-N model, in that it directly influences the enthalpy of mixing and appearence of miscibility gaps (Fig. 5). However, unlike W, J_{FeTi}^{TO} also influences the cation distribution in two distinct ways. Firstly, a positive J_{FeTi}^{TO} drives the system to avoid Fe^{3+}-Ti^{4+} T-O pairs. Since Ti^{4+} is strongly partitioned onto O sites, the system can reduce its total energy by replacing Fe^{3+} on T with Mg^{2+}. This substitution will only occur when the resulting energy reduction outweighs the increase in chemical potential energy (μ_x). The energy balance tips in favour of increased Mg^T for $J_{FeTi}^{TO} \geq 500$ K (Fig. 2). Secondly, a positive J_{FeTi}^{TO} drives the system to chemically cluster and eventually unmix (Fig. 6). In the limit of perfect unmixing into a mechanical mixture of inverse $MgFe_2O_4$ and inverse Mg_2TiO_4, the amount of Mg^{2+} on tetrahedral sites (averaged over the whole simulation cell) would be $Mg^T = M$ (i.e. the Akimoto model). This may help to explain why the system evolves towards the Akimoto model with increasing J_{FeTi}^{TO}, and suggests that the short-range chemical clustering observed in Fig. 6 may be a prerequisite to obtaining the correct cation distribution. Such short-range effects can only be described using the atomistic approach, providing additional motivation for the continued development of such models.

496 *4.2. Outlook*

497 This comparative study of $MgFe_2O_4$-Mg_2TiO_4 and Fe_3O_4-Fe_2TiO_4 has highlighted several
498 issues that need to be more thoroughly investigated before a complete model of the titanomagnetite
499 system can be finalised. The proposed screening mechanism, whereby the electrostatic contribution
500 to certain cation-cation interaction energies can be reduced in proportion to the Fe_3O_4 content of the
501 solid solution, needs to be confirmed. A possible methodology would be to perform detailed first-
502 principles ab initio calculations, where the assumption of discrete Fe^{2+} and Fe^{3+} cations with formal
503 charges can be relaxed and the excess electronic charge can be allowed to distribute itself more
504 naturally across the available Fe sites (Pentcheva and Nabi 2008; Nabi et al. 2010; Skomurski et al.
505 2010). Any new analysis of this type should also investigate in more detail the relative importance
506 of electrostatic versus volume strain contributions to the total energy, so that the final model can
507 reproduce observed cation distributions and enthalpies of mixing simultaneously (Vinograd et al.
508 2004). We have shown that coupling between magnetic and cation ordering will have a small but
509 non-negligible effect on the cation distribution below T_c, and therefore including coupling is a
510 necessary next step in improving the atomistic model. The temperature- and composition-dependent
511 kinetics of Fe^{2+}-Fe^{3+} redistribution in titanomagnetite are poorly constrained. Kinetic effects play a
512 crucial role in understanding the impact of coupling to the magnetic transition and also in helping to
513 explain the large variation in observed cation distributions between different experimental studies.
514 Kinetic studies of synthetic and natural titanomagnetite are, therefore, a crucial area for future
515 experimental work.

516
517 **ACKNOWLEDGEMENTS**

518 This work was supported by the European Science Foundation (ESF) under the EUROCORES
519 program EuroMinScI, through contract number ERAS-CT-2003-980409 of the European
520 Commission, DG Research, FP6 and through NERC grant NE/D522203/1.

521
522 **REFERENCES**

523

524 Andreozzi, G.B. and Lucchesi, S. (2002) Intersite distribution of Fe^{2+} and Mg in the spinel (sensu
525 stricto)–hercynite series by single-crystal X-ray diffraction. American Mineralogist, 87, 1113–1120.

Akimoto, S. (1954) Thermomagnetic study of ferromagnetic minerals contained in igneous rocks. Journal of Geomagnetism and Geoelectricity, 6, 1–14.

Antao, S.M., Hassan, I. and Parise, J.B. (2005) Cation ordering in magnesioferrite, $MgFe_2O_4$ to 982 °C using in situ synchrotron X-ray powder diffraction. American Mineralogist, 90, 219–228.

Bosenick, A., Dove, M.T., Myers, E.R., Palin, E.J., Sainz-Diaz, C.I., Guiton, B.S., Warren, M.C., Craig, M.S. and Redfern, S.A.T. (2001) Computational methods for the study of energies of cation distributions: applications to cation-ordering phase transitions and solid solutions. Mineralogical Magazine, 65, 193–219.

Bosi, F., Hålenus, U. and Skogby, H. (2009) Crystal chemistry of the magnetite-ulvöspinel series. American Mineralogist, 94, 181–189.

Chevalier, R., Bolfa, J. and Mathieu, S. (1955) Titanomagnétites et ilménites ferromagnétiques. Bulletin du Société Français Minéralogie et Cristallographie, 78, 307–346.

Church, N., Feinberg, J. and Harrison, R.J. (2011) Low-temperature domain wall pinning in titanomagnetite. Geochemistry Geophysics Geosystems, 12, Q07Z27, doi:10.1029/2011GC003538.

de Grave, E., de Sitter, J. and Vandenberghe, R. (1975) On the cation distribution in the spinel system $y Mg_2TiO_4$-(1 - y)$MgFe_2O_4$. Applied Physics, 7, 77–80.

Eveno, P. and Paulus, M. (1974) Diffusion of nickel-63 in mixed ferrites of iron and nickel. Physica Status Solidi A, 22, 569–77.

Gale, J.D. (1997) GULP: a computer program for the symmetry-adapted simulation of solids. Journal of the Chemical Society: Faraday Transactions, 93, 629–637.

556 Gale, J.D. and Rohl, A.L. (2003) The general utility lattice program (GULP). Molecular Simulation,
557 29, 291–341.
558
559 Hamdeh, H.H., Barghout, K., Ho, J.C., Shand, P.M. and Miller, L.L. (1999) A Mössbauer
560 evaluation of cation distribution in titanomagnetites. Journal of Magnetism and Magnetic Materials,
561 191, 72–78.
562
563 Harrison, R.J. and Putnis, A. (1997) The coupling between magnetic and cation ordering: A
564 macroscopic approach. European Journal of Mineralogy, 9, 1115-1130.
565
566 Harrison, R.J. and Putnis, A. (1999a) The magnetic properties and crystal chemistry of oxide spinel
567 solid solutions. Surveys in Geophysics, 19, 461–520.
568
569 Harrison, R.J. and Putnis, A. (1999b) Determination of the mechanism of cation ordering in
570 magnesioferrite ($MgFe_2O_4$) from the time- and temperature-dependence of magnetic susceptibility.
571 Physics and Chemistry of Minerals, 26, 322-332.
572
573 Harrison, R.J., Becker, U. and Redfern, S.A.T. (2000) Thermodynamics of the R-3 to R-3c phase
574 transition in the ilmenite-hematite solid solution. American Mineralogist, 85, 1694-1705.
575
576 Harrison, R.J. and Becker, U. (2001) Magnetic ordering in solid solutions. In C. Geiger (ed) "Solid
577 solutions in silicate and oxide systems", European Mineralogical Union Notes in Mineralogy Vol. 3
578 Chapter 13, 349–383.
579
580 Harrison, R.J. (2006) Microstructure and magnetism in the ilmenite-hematite solid solution: a
581 Monte Carlo simulation study. American Mineralogist, 91, 1006–1024.
582
583 Kąkol, Z., Sabol, J. and Honig, J. (1991a) Magnetic anisotropy of titanomagnetites $Fe_{3-x}Ti_xO_4$ $0 \leq x$
584 < 0.55. Physical Review B: Condensed Matter, 44, 2198–2204.
585

586 Kąkol, Z., Sabol, J. and Honig, J. (1991b) Cation distribution and magnetic properties of
587 titanomagnetites $Fe_{3-x}Ti_xO_4$ ($0 \leq x < 1$). Physical Review B: Condensed Matter, 43, 649–654.
588
589 Kimura, T., Ichikawa, M. and Yamaguchi T. (1977) Effects of grain size on cation ordering in
590 sintered Mg-ferrites. Journal of Applied Physics, 48, 5033–5037.
591
592 Lilova, K.I., Pearce, C., Gorski, C., Rosso, K.M. and Navrotsky, A. (2012) Thermodynamics of the
593 magnetite-ulvöspinel (Fe_3O_4-Fe_2TiO_4) solid solution. American Mineralogist, 97, 1330-1338.
594
595 Nabi, H.S., Harrison, R.J. and Pentcheva, R. (2010) Magnetic coupling parameters at an oxide-
596 oxide interface from first principles: Fe_2O_3-$FeTiO_3$. Physical Review B, 81, 214432.
597
598 Néel, L. (1955) Some theoretical aspects of rock-magnetism. Advances in Physics, 54, 191–243.
599
600 Nell, J., Wood, B. and Mason, T.O. (1989) High-temperature cation distributions in Fe_3O_4-
601 $MgAl_2O_4$-$MgFe_2O_4$-$FeAl_2O_4$ spinels from thermopower and conductivity measurments. American
602 Mineralogist, 74, 339–351.
603
604 O'Neill, H.St.C. and Navrotsky, A. (1983) Simple spinels: crystallographic parameters, cation radii,
605 lattice energies, and cation distribution. American Mineralogist, 68, 181–194.
606
607 O'Neill, H.St.C. and Navrotsky, A. (1984) Cation distributions and thermodynamic properties of
608 binary spinel solid solutions. American Mineralogist, 69, 733–753.
609
610 O'Neill, H.St.C., Annersten, H. and Virgo, D. (1992) The temperature dependence of the cation
611 distribution in magnesioferrite ($MgFe_2O_4$) from powder XRD structural refinements and Mössbauer
612 spectroscopy. American Mineralogist, 77, 725–740.
613

O'Neill, H.St.C., Redfern, S.A.T., Kesson, S. and Short, S. (2003) An in situ neutron diffraction study of cation disordering in synthetic qandilite Mg_2TiO_4 at high temperatures. American Mineralogist, 88, 860–865.

Palin, E.J. and Harrison, R.J. (2007a) A computational investigation of cation ordering phenomena in the binary spinel system $MgAl_2O_4$-$FeAl_2O_4$. Mineralogical Magazine, 71, 611–624.

Palin, E.J. and Harrison, R.J. (2007b) A Monte Carlo investigation of the thermodynamics of cation ordering in 2-3 spinels. American Mineralogist, 92, 1334–1345.

Palin, E.J., Walker, A.M. and Harrison, R.J. (2008) A computational study of order-disorder phenomena in Mg_2TiO_4 spinel (qandilite). American Mineralogist, 93, 1363–1372.

Pearce, C., Henderson, C.M.B, Telling, N.D., Pattrick, R.A.D., Charnock, J.M., Coker, V.S, Arenholz, E., Tuna, F. and van der Laan, G. (2010) Fe site occupancy in magnetite-ulvöspinel solid solutions: A new approach using X-ray magnetic circular dichroism. American Mineralogist, 95, 425–439.

Pentcheva, R. and Nabi, H.S. (2009) Interface magnetism in Fe_2O_3/$FeTiO_3$ heterostructures. Physical Review B, 77, 172405.

Price, G.D. (1981) Subsolidus phase relations in the titanomagnetite solid solution series. American Mineralogist 66, 751–758.

Sack, R.O. and Ghiorso, M.S. (1991) An internally consistent model for the thermodynamic properties of Fe-Mg-titanomagnetite-aluminate spinels. Contributions to Mineralogy and Petrology, 106, 474–505.

642 Skomurski, F.N., Kerisit, S.N., and Rosso, K.M. (2010) Structure, charge distribution, and electron
643 hopping dynamics in magnetite (Fe_3O_4) (100) surfaces from first principles. Geochimica et
644 Cosmochimica Acta 74, 4234-4248.
645
646 Sujata, K. and Mason, T.O. (1992) Kinetics of Cation Redistribution in Ferrospinels. Journal of the
647 American Ceramic Society, 75, 557–562.
648
649 Tellier, J.C. (1967) Sur la substitution dans le ferrite de magnésium des ions ferriques par les ions
650 trivalents, tetravelant et pentavalent. Revue de Chimie Minerale, 4, 325–365.
651
652 Trestman-Matts, A., Dorris, S.E., Kumarakrishnan, S. and Mason, T.O. (1983) Thermoelectric
653 determination of cation distributions in Fe_3O_4-Fe_2TiO_4. Journal of the Americal Ceramic Society,
654 66, 829–834.
655
656 Trestman-Matts, A., Dorris, S.E. and Mason, T.O. (1984) Thermoelectric determination of cation
657 distributions in Fe_3O_4-$MgFe_2O_4$. Journal of the Americal Ceramic Society, 67, 69–73.
658
659 Vinograd, V.L., Sluiter, M.H.F., Winkler, B., Putnis, A., Hålenius, U., Gale, J.D. and Becker, U.
660 (2004) Thermodynamics of mixing and ordering in pyrope-grossular solid solution. Mineralogical
661 Magazine, 68, 101–121.
662
663 Walters, D.S. and Wirtz, G.P. (1971) Kinetics of cation ordering in magnesium ferrite. Journal of
664 the American Ceramic Society, 54, 563–566.
665
666 Wißmann, S., Wurmb, V. v., Litterst, F.J., Dieckmann, R. and Becker, K.D. (1998) The
667 temperature-dependent cation distribution in magnetite. Journal of Physics and Chemistry of Solids
668 59, 321–330.
669
670 **FIGURE CAPTIONS**

671

Figure 1. Cation-cation interaction energies extracted from static lattice energy calculations using the optimisation procedure of Bosenick et al. (2001). J_1, J_2, J_3 and J_4 refer to 1st, 2nd, 3rd and 4th nearest neighbour interactions. TT, OO and TO refer to tetrahedral-tetrahedral, octahedral-octahedral and tetrahedral-octahedral interactions, respectively. TT interactions involving Ti^{4+} are absent, since Ti^{4+} was placed on octahedral sites only.

Figure 2. Summary of MC results obtained for $MgFe_2O_4$-Mg_2TiO_4 with J_{FeTi}^{TO} equal to (a) 0 K, (b) 250 K, (c) 500 K, (d) 750 K, (e) 850 K, (f) 1000 K, (g) 1100 K, (h) 1250 K and (i) 1500 K. Solid curves show the results of MC simulations performed at temperatures of (from upper to lower curves) 1750 K, 1500 K, 1250 K, 1000 K, 750 K, 500 K and 250 K. Dashed lines show reference cation distribution models (from upper to lower dashed curves): Random, Akimoto, Kąkol and Néel-Chevalier.

Figure 3. (a) Experimentally determined cation distributions in $MgFe_2O_4$-Mg_2TiO_4. Open circles are data from this study. Triangles are quenched and slowly cooled samples from de Grave et al. (1975). (b) Experimentally determined cation distributions in Fe_3O_4-Fe_2TiO_4. Data are from Bosi et al. (2009) (circles), Hamdeh et al. (1999) (squares), Lilova et al. (2012) (upward triangles) and Pearce et al. (2010) (downward triangles). Solid lines in (a) and (b) show reference cation distribution models (from upper to lower): Random, Akimoto, Kąkol and Néel-Chevalier.

Figure 4. (a) Cation distributions in $MgFe_2O_4$-Mg_2TiO_4 plotted in the form of Eqn. 3 (O'Neill and Navrotsky 1984). Data shown from this study (open circles), Tellier (1967) (closed squares) and de Grave et al. (1975) (open triangles). Solid curves show the results of MC simulations with J_{FeTi}^{TO} = 1000 K at temperatures of (from lower to upper curves) 1750 K, 1500 K, 1250 K, 1000 K, 750 K, 500 K and 250 K. Dashed line shows the prediction of the O'Neill and Navrotsky (1984) model using Eqn. 3 with values of α = 26.6 kJ/mol and β = -21.7 kJ/mol (O'Neill et al. 1992). (b) Direct comparison of observed cation distributions in $MgFe_2O_4$-Mg_2TiO_4 with results of MC simulations with J_{FeTi}^{TO} = 1000 K at temperatures of (from upper to lower curves) 1750 K, 1500 K, 1250 K, 1000 K, 750 K, 500 K and 250 K.

Figure 5. Enthalpy of mixing for $MgFe_2O_4$-Mg_2TiO_4 calculated from MC simulations with J_{FeTi}^{TO} = 1000 K at temperatures of (from upper to lower curves) 1750 K, 1500 K, 1250 K, 1000 K, 750 K, 500 K and 250 K. For comparison, data points show the measured enthalpy of mixing for Fe_3O_4-Fe_2TiO_4 (Lilova et al. 2012).

Figure 6. Snapshots of the final configuration of MC simulations performed for M = 0.5 and T = (a) 1750 K, (b) 1000 K, (c) 750 K and (d) 250 K. Mg^{2+} is red, Fe^{3+} is green and Ti^{4+} is blue. View direction is [111].

Figure 7. Prediction of how the degree of inversion (x = Fe^{3+} on tetrahedral sites) is influenced by the onset of magnetic ordering in an inverse spinel with cation ordering behaviour that is similar to $MgFe_2O_4$ but with magnetic ordering behaviour that is similar to Fe_3O_4. Thin dashed line (left axis) shows cation ordering behaviour in the absence of coupling. Thick solid curve (left axis) shows the predicted behaviour with coupling. Thin solid curve (right axis) shows the magnetic order parameter (Q_m).

Figure 8. (a) Optimisation of the atomistic model to reproduce the Kąkol model for Fe_3O_4-Fe_2TiO_4 (Kąkol et al. 1991b). Thin solid curves show the results of MC simulations with a value of J_{FeTi}^{TO} that varies with composition according to the inset (solid circles). Simulations were performed for temperatures of (from upper to lower curves) 1750 K, 1500 K, 1250 K, 1000 K, 750 K, 500 K and 250 K. Data are from Bosi et al. (2009) (circles), Hamdeh et al. (1999) (squares), Lilova et al. (2012) (upward triangles) and Pearce et al. (2010) (downward triangles). Thick solid lines show reference cation distribution models (from upper to lower): Random, Akimoto, Kąkol and Néel-Chevalier. Open circles in the inset show values of J_{FeTi}^{TO} that are needed to fit the data of Pearce et al. (2010). (b) Calculated enthalpy of mixing for Fe_3O_4-Fe_2TiO_4 using the cation distribution model from (a). Data points show the measured enthalpy of mixing for Fe_3O_4-Fe_2TiO_4 (Lilova et al. 2012).

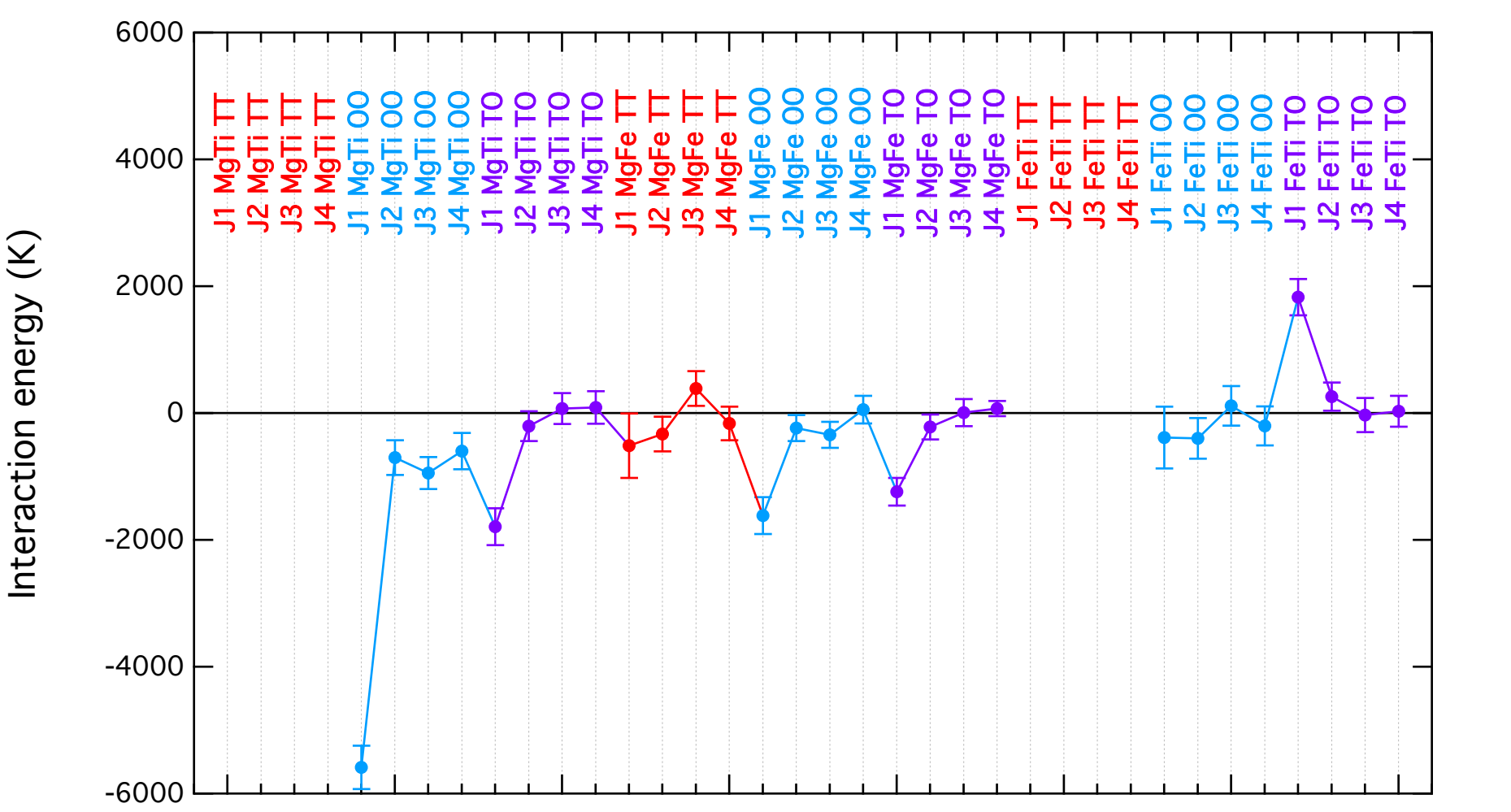
Interaction energy (K)
6000
4000
2000
0
-2000
-4000
-6000
J1 MgTi TT
J2 MgTi TT
J3 MgTi TT
J4 MgTi TT
J1 MgTi OO
J2 MgTi OO
J3 MgTi OO
J4 MgTi OO
J1 MgTi TO
J2 MgTi TO
J3 MgTi TO
J4 MgTi TO
J1 MgFe TT
J2 MgFe TT
J3 MgFe TT
J4 MgFe TT
J1 MgFe OO
J2 MgFe OO
J3 MgFe OO
J4 MgFe OO
J1 MgFe TO
J2 MgFe TO
J3 MgFe TO
J4 MgFe TO
J1 FeTi TT
J2 FeTi TT
J3 FeTi TT
J4 FeTi TT
J1 FeTi OO
J2 FeTi OO
J3 FeTi OO
J4 FeTi OO
J1 FeTi TO
J2 FeTi TO
J3 FeTi TO
J4 FeTi TO

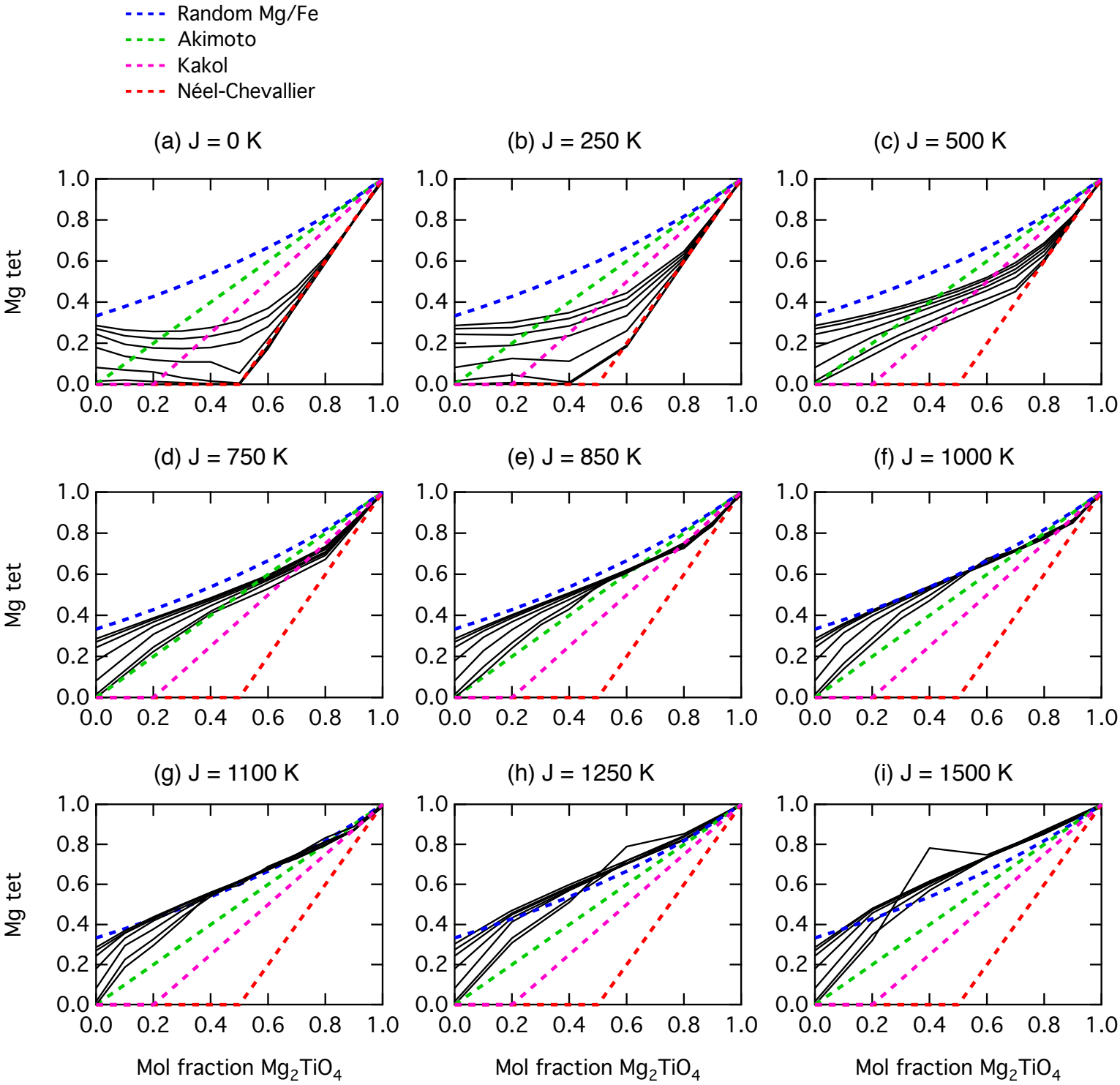
Random Mg/Fe
Akimoto
Kakol
Néel-Chevallier
(a) J = 0 K
(b) J = 250 K
(c) J = 500 K
(d) J = 750 K
(e) J = 850 K
(f) J = 1000 K
(g) J = 1100 K
(h) J = 1250 K
(i) J = 1500 K
Mg tet
Mol fraction Mg_2TiO_4
0.0
0.2
0.4
0.6
0.8
1.0

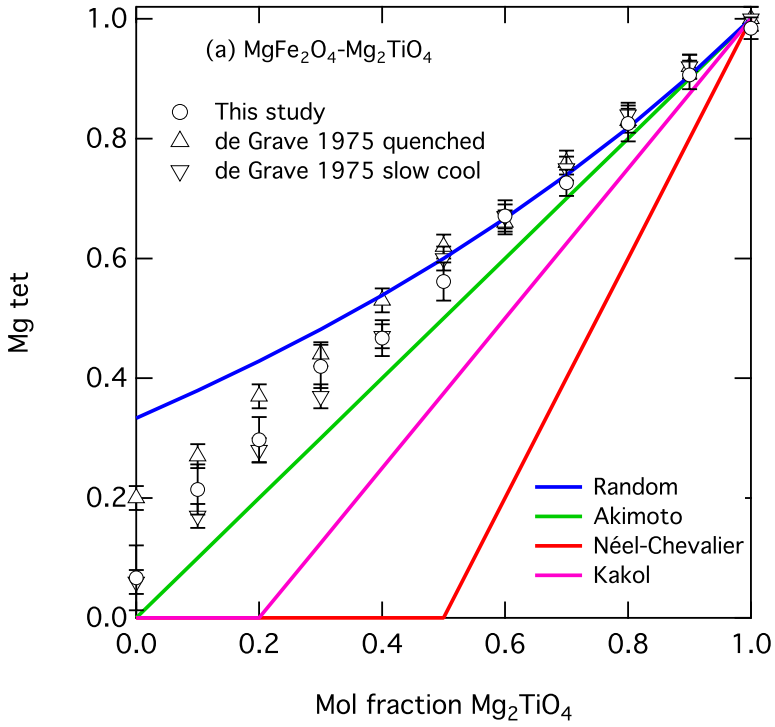
(a) MgFe2O4-Mg2TiO4
This study
de Grave 1975 quenched
de Grave 1975 slow cool
Random
Akimoto
Néel-Chevalier
Kakol
Mg tet
Mol fraction Mg2TiO4
0.0
0.2
0.4
0.6
0.8
1.0

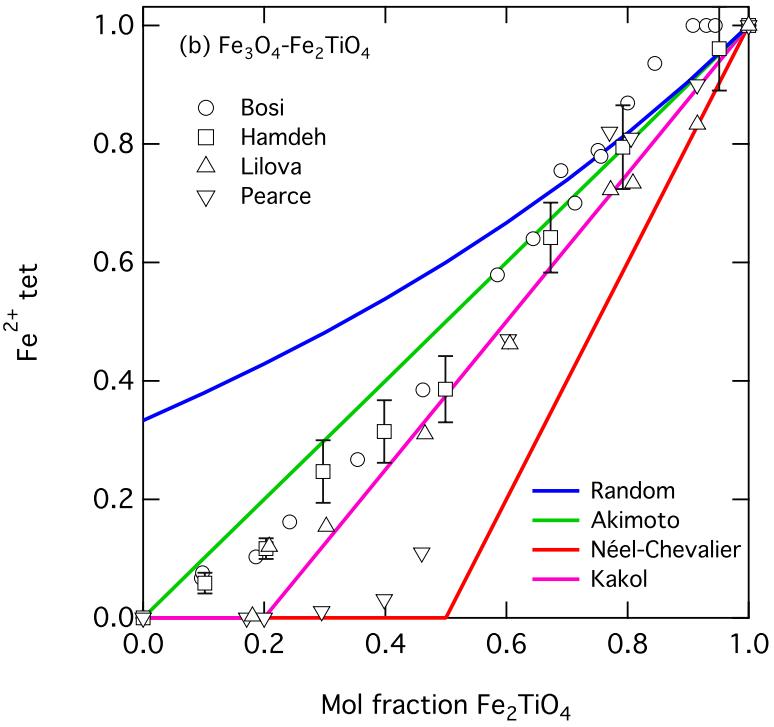
(b) Fe3O4-Fe2TiO4
Bosi
Hamdeh
Lilova
Pearce
Random
Akimoto
Néel-Chevalier
Kakol
Fe2+ tet
Mol fraction Fe2TiO4
0.0
0.2
0.4
0.6
0.8
1.0

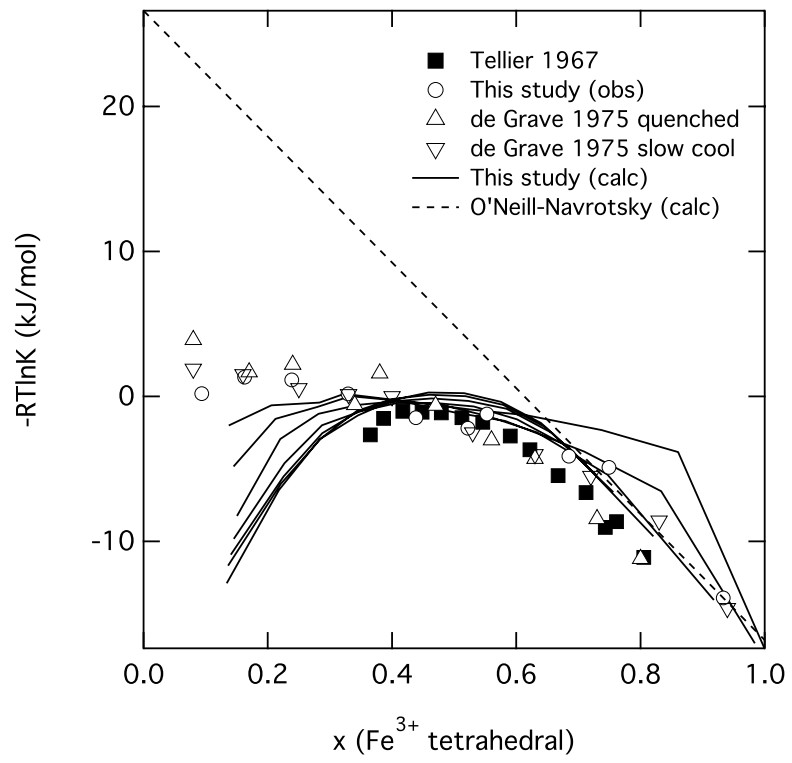
Tellier 1967
This study (obs)
de Grave 1975 quenched
de Grave 1975 slow cool
This study (calc)
O'Neill-Navrotsky (calc)
-RTlnK (kJ/mol)
x (Fe3+ tetrahedral)
20
10
0
-10
0.0
0.2
0.4
0.6
0.8
1.0

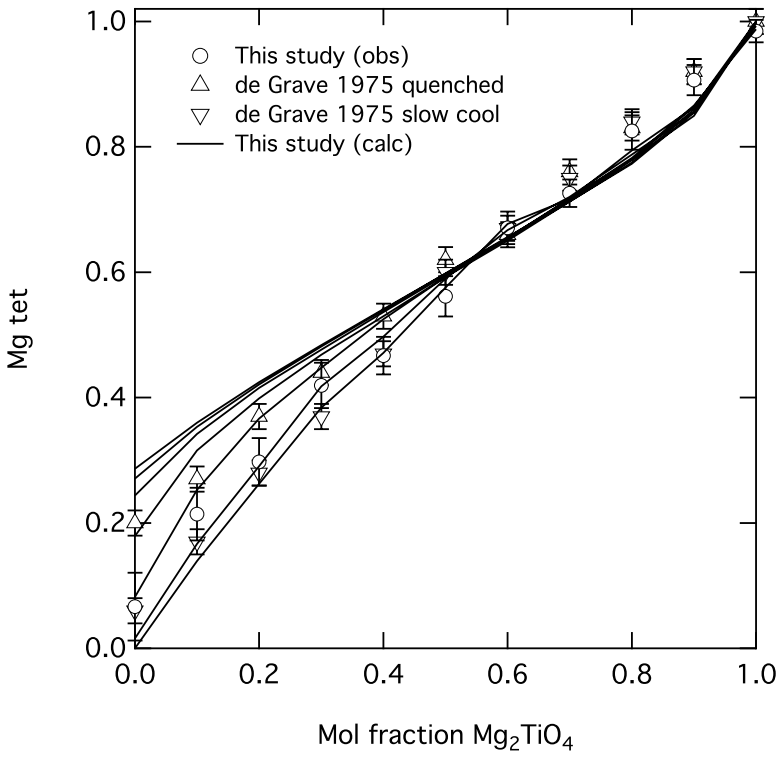
This study (obs)
de Grave 1975 quenched
de Grave 1975 slow cool
This study (calc)
Mg tet
Mol fraction Mg2TiO4
1.0
0.8
0.6
0.4
0.2
0.0
0.0
0.2
0.4
0.6
0.8
1.0

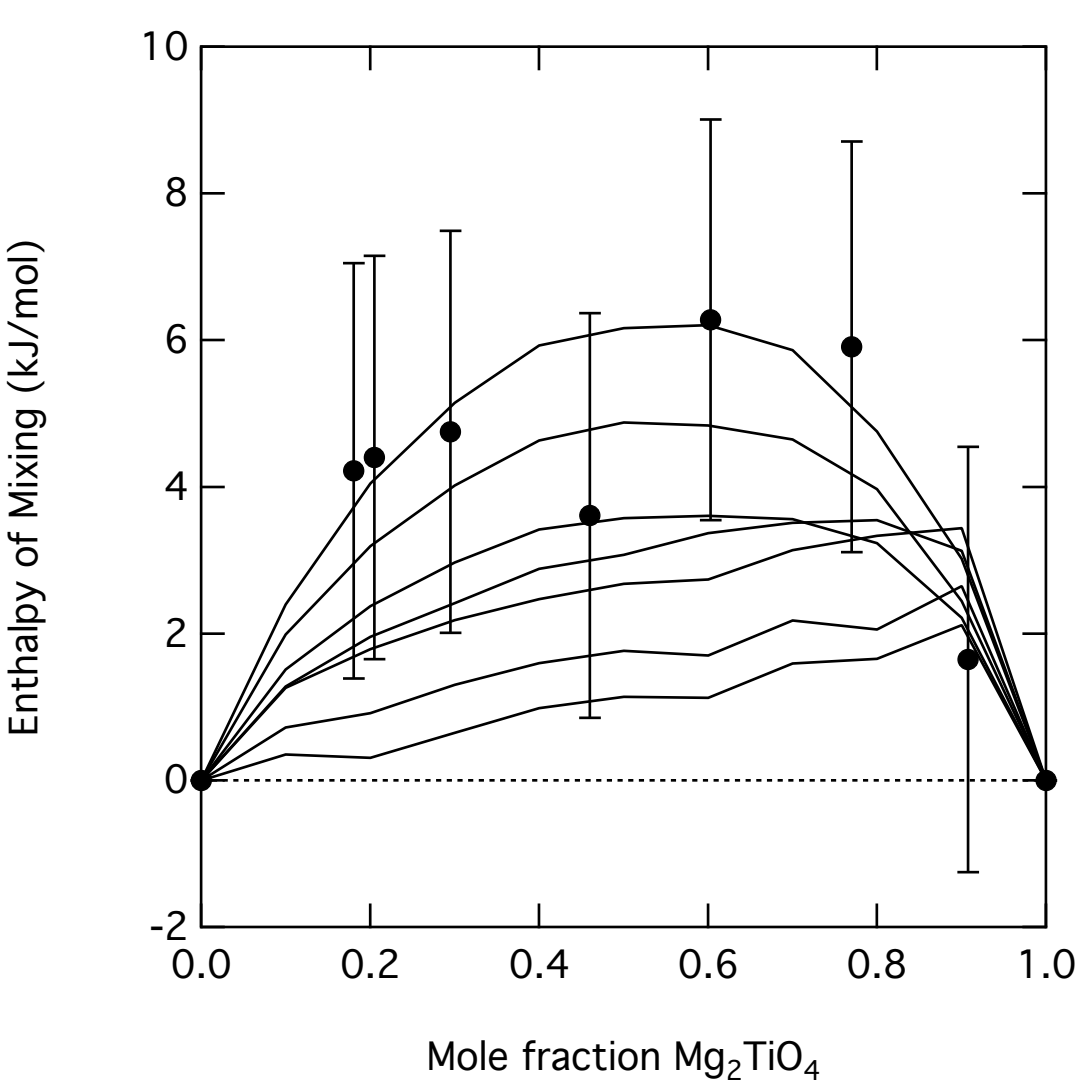
10
8
6
4
2
0
-2
0.0
0.2
0.4
0.6
0.8
1.0
Enthalpy of Mixing (kJ/mol)
Mole fraction Mg_2TiO_4

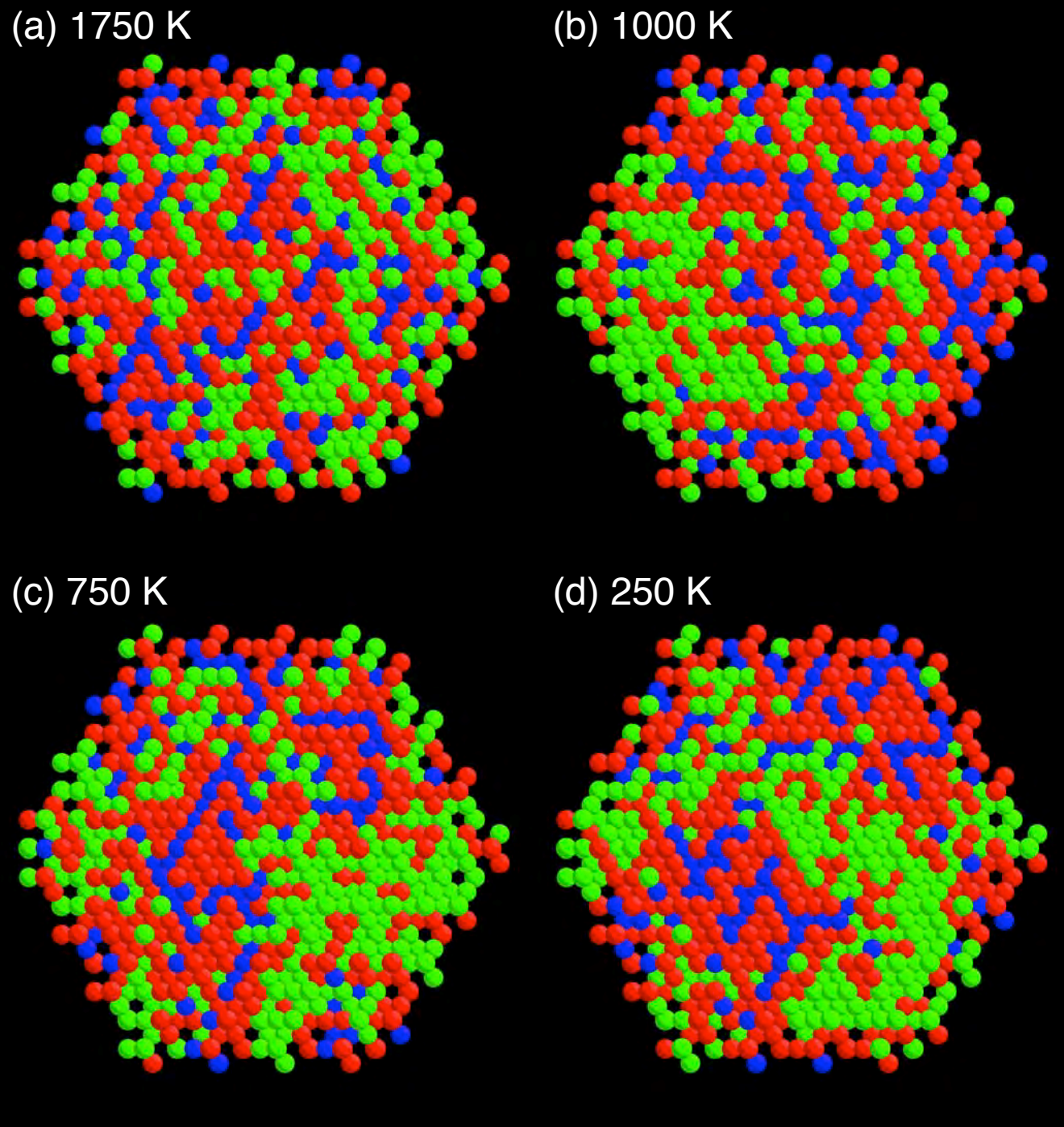
(a) 1750 K
(b) 1000 K
(c) 750 K
(d) 250 K

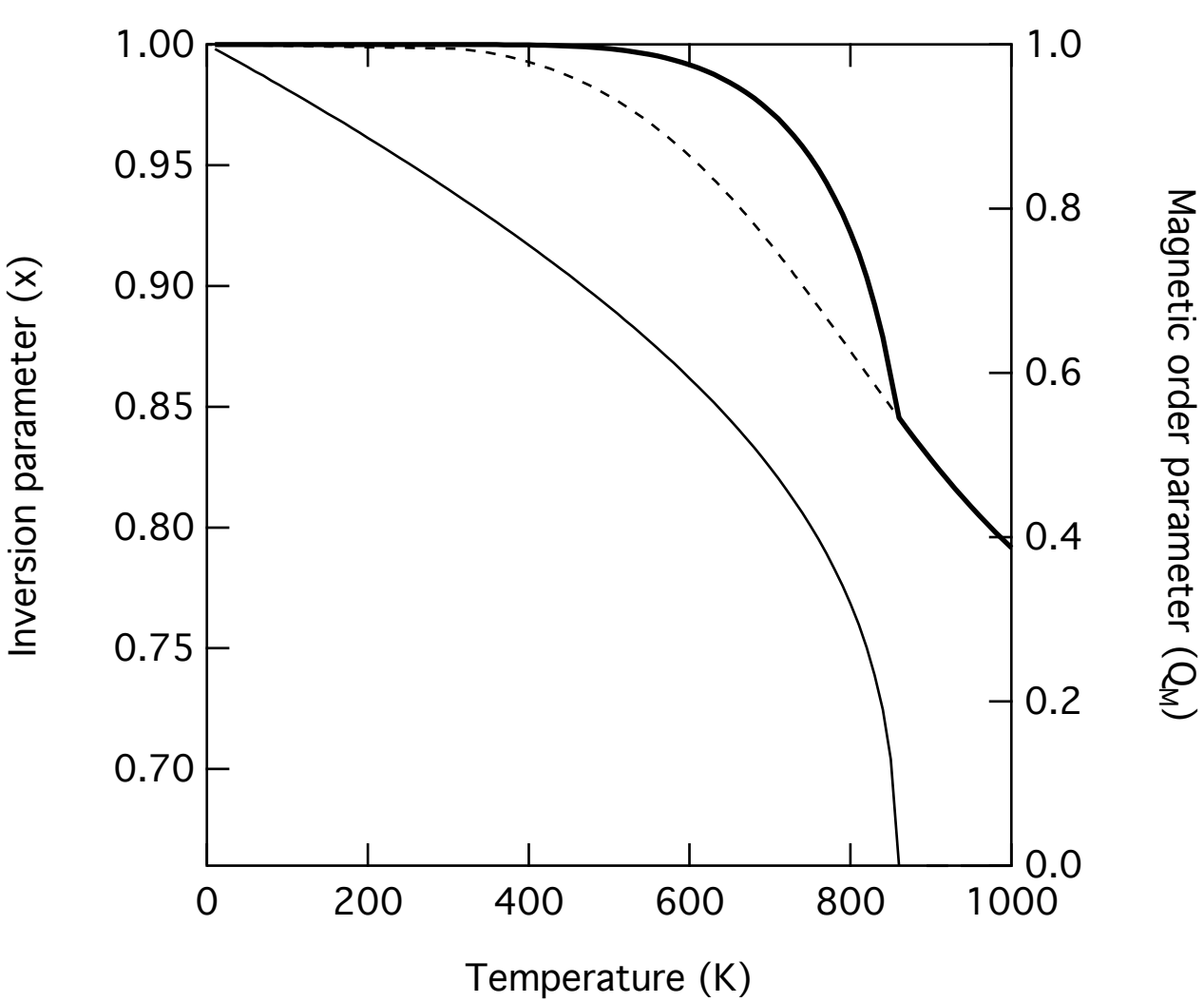
1.00
0.95
0.90
0.85
0.80
0.75
0.70
Inversion parameter (x)
1.0
0.8
0.6
0.4
0.2
0.0
Magnetic order parameter (Q_M)
0
200
400
600
800
1000
Temperature (K)

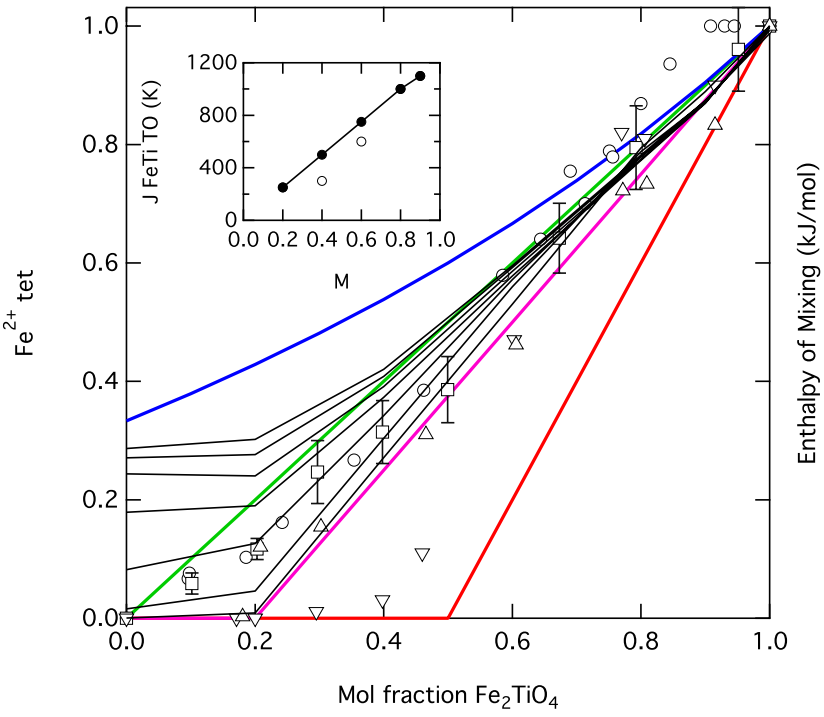
1.0
0.8
0.6
0.4
0.2
0.0
0.0
0.2
0.4
0.6
0.8
1.0
Fe2+ tet
Mol fraction Fe2TiO4
J FeTi TO (K)
1200
800
400
0
0.0 0.2 0.4 0.6 0.8 1.0
M

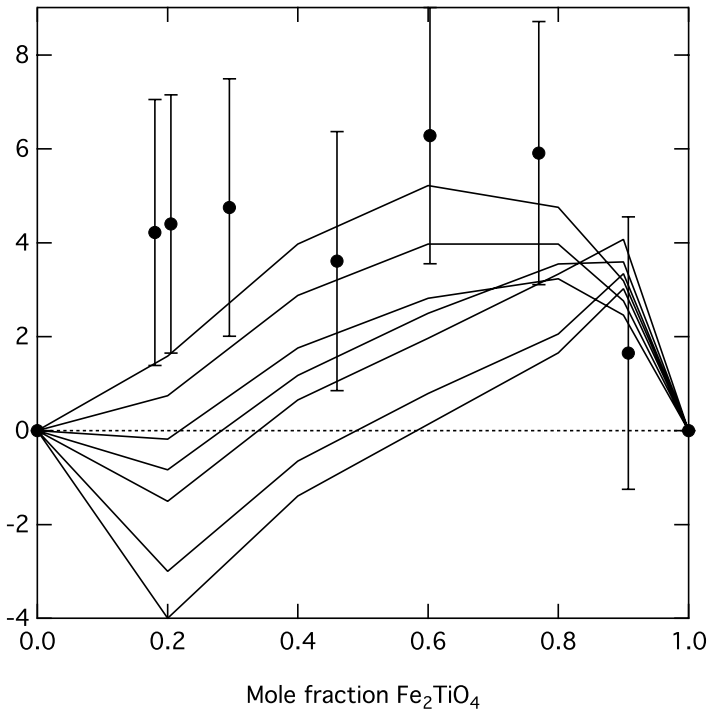
8
6
4
2
0
-2
-4
0.0
0.2
0.4
0.6
0.8
1.0
Enthalpy of Mixing (kJ/mol)
Mole fraction Fe2TiO4

Table 1. Cation-cation interaction parameters and chemical potentials of the atomistic model

	Energy (K)	Reference
J1 MgTi TT	728	Palin et al. (2008)
J2 MgTi TT	0	Palin et al. (2008)
J3 MgTi TT	0	Palin et al. (2008)
J4 MgTi TT	0	Palin et al. (2008)
J1 MgTi OO	-3102	Palin et al. (2008)
J2 MgTi OO	0	Palin et al. (2008)
J3 MgTi OO	-272	Palin et al. (2008)
J4 MgTi OO	-116	Palin et al. (2008)
J1 MgTi TO	-1706	Palin et al. (2008)
J2 MgTi TO	0	Palin et al. (2008)
J3 MgTi TO	0	Palin et al. (2008)
J4 MgTi TO	0	Palin et al. (2008)
J1 MgFe TT	-164	Palin and Harrison (2007a)
J2 MgFe TT	-68	Palin and Harrison (2007a)
J3 MgFe TT	-45	Palin and Harrison (2007a)
J4 MgFe TT	-5	Palin and Harrison (2007a)
J1 MgFe OO	-340	Palin and Harrison (2007a)
J2 MgFe OO	-51	Palin and Harrison (2007a)
J3 MgFe OO	-62	Palin and Harrison (2007a)
J4 MgFe OO	-28	Palin and Harrison (2007a)
J1 MgFe TO	-313	Palin and Harrison (2007a)
J2 MgFe TO	-144	Palin and Harrison (2007a)
J3 MgFe TO	-53	Palin and Harrison (2007a)
J4 MgFe TO	-19	Palin and Harrison (2007a)
J1 FeTi TO	0-1500	This Study
μ_x	-950	Palin and Harrison (2007a)
μ_y	-1114	Palin et al. (2008)